

The Structure of Cucumber Mosaic Virus: Cryoelectron Microscopy, X-Ray Crystallography, and Sequence Analysis

William R. Wikoff,*†¹ Chao Jo Tsai,†¹ Guoji Wang,†² Timothy S. Baker,† and John E. Johnson*³

*Department of Molecular Biology, The Scripps Research Institute, 10550 North Torrey Pines Road, La Jolla, California 92037; and †Department of Biological Sciences, Purdue University, West Lafayette, Indiana 47907

Received November 27, 1996; returned to author for revision December 17, 1996; accepted March 17, 1997

The three-dimensional structure of cucumber mosaic virus (CMV) was analyzed at 23 Å resolution by cryoelectron microscopy and image reconstruction, demonstrating structural similarity to cowpea chlorotic mottle virus (CCMV), another member of the *Bromoviridae* family. The CMV structure was determined at 8 Å resolution by X-ray crystallography with phases determined by single isomorphous replacement and refined by fivefold noncrystallographic symmetry averaging. The X-ray structure agreed with the electron microscopy reconstruction; the electron density is consistent with β -barrel subunits arranged with $T = 3$ quasi-symmetry in an orientation similar to that observed in CCMV. Strong density surrounding the icosahedral threefold axes (quasi sixfold axes in the $T = 3$ particle) between 80 and 100 Å from the particle center formed a cylinder of radius 11 Å, similar to the density observed in the same region of CCMV. This density corresponds to the β -annulus of CCMV, which differentiates hexamers from pentamers and determines the formation of the $T = 3$ particles. The CMV and CCMV amino acid sequences were aligned, providing information (based on the CCMV atomic model) about the probable distribution of residues in the three-dimensional structure of CMV. © 1997 Academic Press

INTRODUCTION

Virions in the *Bromoviridae* family (Murphy *et al.*, 1995) are stabilized with a variety of forces. Cowpea chlorotic mottle virus (CCMV), in the genus *Bromovirus*, can form empty $T = 3$ particles when protein subunits are assembled *in vitro* in the presence of divalent metal ions at neutral pH or at pH 3.0 in the absence of metal ions (Bancroft, 1970). Cucumber mosaic virus (CMV), in the *Cucumovirus* genus, is structurally similar to CCMV, but cannot assemble *in vivo* or *in vitro* without RNA. Nevertheless, protein–protein interactions dictate the formation of hexamers and pentamers in both CCMV and CMV. The degradation of the encapsidated CMV RNA by ribonuclease (Francki, 1968) suggests that the protein subunits are loosely packed or that the capsids are unstable. Subunits in the alfamovirus genus can form hexamers and pentamers and will coat RNA or DNA; they form $T = 1$ particles when the basic amino termini of the subunits are removed or if the subunits are assembled in the presence of pyrophosphate (Yusibov *et al.*, 1996). Among the *Bromoviridae*, the weakest protein–protein interactions occur in ilarvirus particles where subunits have insufficient mutual affinity to form an icosahedral particle under any condition investigated. When the ilarvirus subunits are released from the genomic RNA by proteolytically cleaving the capsid protein *in situ* at Arg

87, they will form only soluble dimers even at high concentrations (Sehnke and Johnson, 1993).

The analysis presented in this report shows that CMV and CCMV virions are similar in: (1) particle morphology, (2) size and orientation of the subunit β -barrels, (3) stabilizing interactions for hexamer formation, and (4) subunit primary sequence. By considering these similarities in the context of the known high-resolution structure of CCMV (Speir *et al.*, 1995), a structural rationale for CMV mutational studies is proposed.

MATERIALS AND METHODS

Three CMV strains (Fny, Y, and O) were propagated in Christie hybrid tobacco plants (*Nicotiana glutinosa* × *Nicotiana clevelandii*) and purified using the protocol of Lot *et al.* (1972). A purification protocol without high-speed centrifugation was also used in an attempt to produce better quality crystals (Speir *et al.*, 1993).

CMV samples were flash-frozen and analyzed by cryoelectron microscopy (cryoEM) and image processing using methods previously described (Cheng *et al.*, 1992; Smith *et al.*, 1993; Baker *et al.*, 1991). Images were recorded at ×49,000 nominal magnification under minimal dose conditions (<20 electrons/Å²). Twenty virion images were used to calculate the reconstruction of CMV at 23 Å.

Three strains of CMV were crystallized by hanging-drop vapor diffusion techniques (McPherson *et al.*, 1982). Crystallization was optimized by screening a wide variety of conditions.

¹ These authors are joint first authors.

² Present address: University of Pittsburgh School of Medicine, Department of Pathology, Scaife Hall Room 5-790, Pittsburgh, PA 15261.

³ To whom correspondence should be addressed.

Diffraction data on X-ray films were collected by oscillation photography at the Cornell High Energy Synchrotron Source (CHESS) F-1 station (wavelength = 0.914 Å, crystal-to-film distance = 210 mm). Most film data were recorded with a 0.5° oscillation angle and 36–50 sec of exposure time. X-ray films were scanned on an Optronics rotating drum scanner with a 50- μ m raster step and indexed using the auto-indexing algorithm developed by Kabsch (1988a). Film data were processed, scaled, and postrefined with the Purdue oscillation film processing (Rossmann, 1979) and scaling and postrefinement programs (Rossmann *et al.*, 1979).

Diffraction data between 100 and 5 Å resolution were collected on a Siemens multiwire area detector with an Elliot GX-20 rotating anode X-ray generator, CuK α radiation, and a nickel-coated double mirror focusing system. Each frame was collected with a 0.05° oscillation angle and 300 to 800 sec of exposure time. Reflections were indexed and processed with the XDS package (Kabsch, 1988a). Individual data sets from different crystals were scaled and merged with the XSCALE program (Kabsch, 1988b). The film and area detector data were combined using a program from Mathur R. N. Murthy (personal communication).

The program CLUSTAL V was used for sequence alignments (Higgins *et al.*, 1992). CCMV, BMV, and BBMV coat proteins were aligned using fixed and floating gap penalties of 10. CMV, peanut stunt virus (PSV), and tomato aspermy virus (TAV) were aligned using the same parameters. The two genera were then aligned to each other using a profile alignment method with the same gap penalties. The PAM250 matrix was used throughout. Calculation of similarity scores and sequence formatting was performed with the GCG package (Genetics Computer Group, 1992). A separate alignment of CMV, PSV, and TAV was used for the secondary structure prediction. Prediction was performed using the neural network profile method PHD (Rost and Sander, 1993, 1994; Rost *et al.*, 1994).

RESULTS AND DISCUSSION

The cryoEM structure displayed prominent pentameric and hexameric morphological units that protrude 40–50 Å beyond the main capsid shell (Fig. 1). The subunits for the pentamers fold toward the fivefold axes at the virus exterior to form a compact structure with density sealing the fivefold axes. In contrast, the hexameric capsomers exhibited large, open holes along the quasi-sixfold axes, creating a channel through the protein shell. Small extensions of density near the quasi-threefold axes connected the individual capsomers. The RNA was packed tightly against the protein shell, leaving a hollow core of about 110 Å along the threefold axes (Fig. 1).

Crystals of CMV exhibited a rhombic dodecahedral morphology and grew to 0.7 mm. They were obtained by

mixing a CMV solution at 10 mg/ml with an equal volume of 50 mM Tris, 0.3 M ammonium sulfate, pH 8.5, buffer in the drop and equilibrated against 0.5 M ammonium sulfate solution in the reservoir at room temperature. Crystals with the same morphology and of the same diffraction quality (~6–5 Å resolution) could also be obtained with HEPES or borate buffers between pH 7.5 and pH 8.7, or with ammonium acetate as the precipitant. They diffracted X-rays to 5 Å resolution with synchrotron radiation and to 6 Å with a rotating anode X-ray source. The CMV crystals belonged to the cubic space group *I*23 with the unit cell parameter $a = 336.0$ Å. The Matthews coefficient (V_m) for CMV crystals was 3.7 Å³ per dalton (Matthews, 1968) assuming two virus particles per unit cell. These parameters dictated only fivefold noncrystallographic symmetry in the unit cell and that the particle position and orientation were fixed by the space group symmetry.

Partial native data sets were measured with synchrotron radiation on photographic film and with a laboratory X-ray source equipped with a multiwire area detector. The film and area detector data sets were combined to generate a composite native set described in Table 1. The phases were initially determined with a cryoEM-based model and, following refinement by noncrystallographic symmetry, they were used to determine heavy atom positions. Several initial models were generated by fitting the atomic coordinates of CCMV into the CMV cryoEM reconstructed density. The initial *R* factor for the best model tested, which had 30% fewer amino acids than the CMV coat protein, was 54% for data between 100 and 6 Å. After nine cycles of phase extension, which began with data between 100 and 14 Å resolution and ended with data between 100 and 9.8 Å resolution, and a total of 66 cycles of averaging, the final mean correlation coefficient and the *R* factor reached 0.87 and 20.6%, respectively, between 100 and 9.8 Å. The final phases changed an average of 62° from the original model phases.

FMA derivative crystals were produced by soaking the native CMV crystals in 0.25 to 1 mM fluorescein mercuric acetate (FMA, FW = 849.6) dissolved in the synthetic mother liquor (either 0.5 M ammonium sulfate or 1.0 M ammonium acetate in 50 mM Tris buffer at pH 8.5 depending on the precipitant used for crystallization) for 12 to 48 hr. A drop of heavy atom solution was placed next to the crystal drop to allow slow diffusion into the crystal and minimize crystal cracking. A derivative data set from 100 to 8 Å was collected on a Siemens area detector for a total of 5475 unique reflections (Table 2), with an overall completeness of 40% for data with $I > 3\sigma(I)$. The heavy atom sites for the FMA derivative were determined from an averaged difference Fourier map computed with the refined molecular replacement phases described above. The FMA coordinates and relative occupancies were refined to convergence with fixed temperature factors of

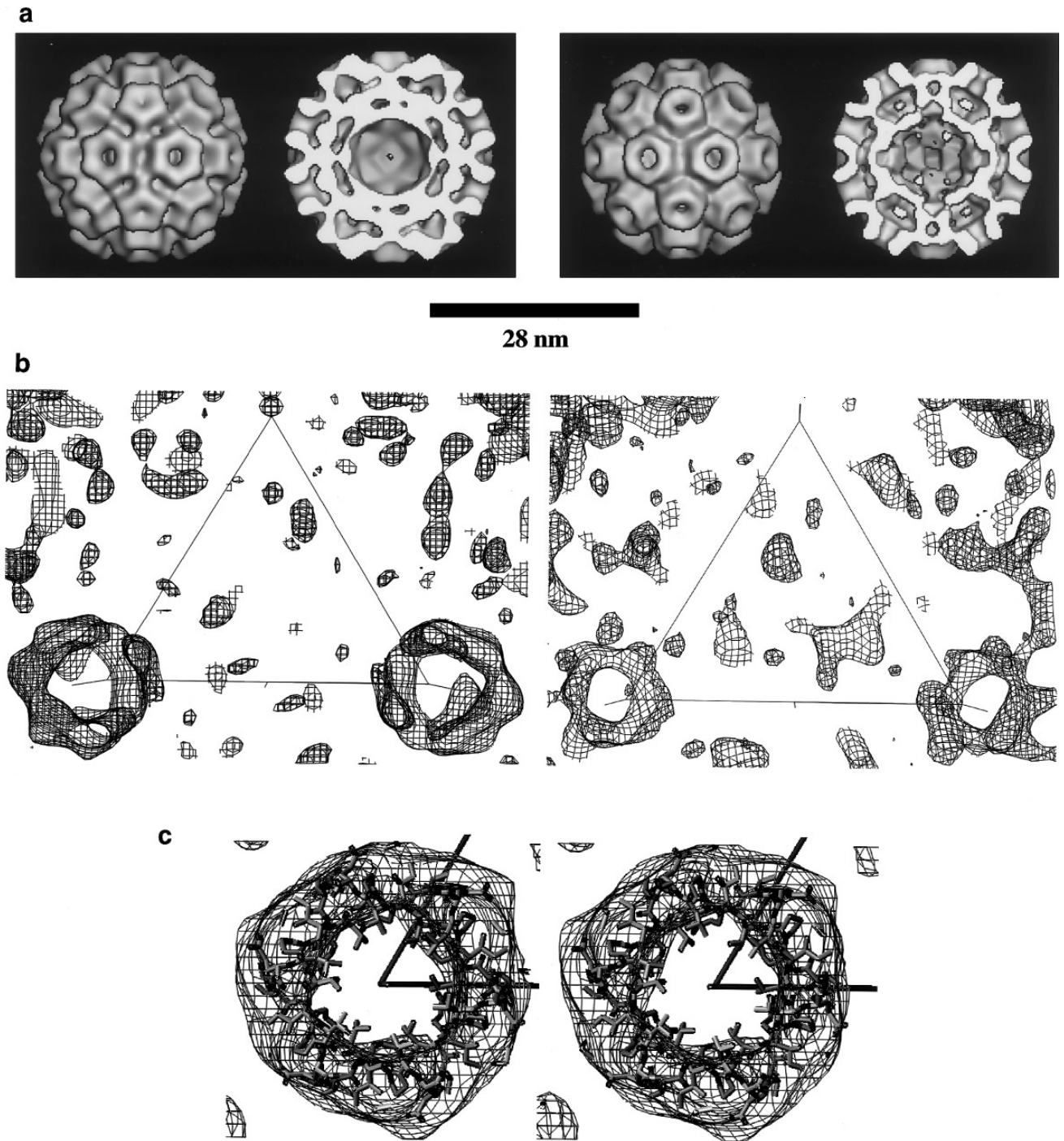


FIG. 1. (a) CryoEM image reconstructions of frozen-hydrated CMV (left) and CCMV (right) samples at 23 Å resolution. The particles are oriented with a twofold axis perpendicular to the plane of the page. For both viruses, a view of the exterior (left) and a vertical slice through the center of the particle (right) to reveal internal features are shown. CMV and CCMV are composed of distinct pentameric and hexameric morphological units arranged with $T = 3$ symmetry. The outer radial dimension of the hexamers are 145 Å for CMV and 138 Å for CCMV. Bar, 280 Å. (b) An internal region of the electron density maps determined by X-ray crystallography at 8 Å of CMV (left) and CCMV (right). The polypeptide occupying this region of the electron density in CCMV (residues 29–33) is part of the molecular switch that determines the formation of hexamers and pentamers and nearly identical density is found for CMV, indicating that the two viruses share mechanisms for determining quasi-equivalence. The density is 22 Å thick for CMV and 18 Å for CCMV and cut perpendicular to the twofold axis. The maps are oriented identically as in (a) with the twofold axis at the bottom center, threefold at the bottom left and right, and the fivefold at the top center. The β -hexamer feature has an outer radius of 111 Å in CMV and 108 Å in CCMV. The base of the triangle defining the asymmetric unit is 65 Å. (c) Stereo pair, showing the β -hexamer feature in the 8 Å CMV map at the left vertex of the CMV density in (b) with the edges of the triangle are shown for reference. The atomic coordinates for residues 29 to 33 of the CCMV hexamer related subunits are also shown. These coordinates were skewed into the CMV unit cell, but were otherwise unchanged.

TABLE 1

A Summary of Reflections Measured after Combining the Film and Area Detector Data Sets

Resolution (Å)	Percentage of theoretically observable data	Number of unique reflections
99–20.0	94	405
20–17.0	100	268
17–15.0	100	321
15–13.0	100	548
13–11.0	98	989
11–10.0	98	833
10–9.0	94	1,210
9–8.0	87	1,714
8–7.0	75	2,506
7–6.0	65	3,825
Total: 99–6.0	82.2	12,784

20.0 (Table 3) using the heavy atom least-squares phasing and refinement program with noncrystallographic constraints (Rossmann, 1976). The heavy atom sites obeyed the expected quasi-symmetry for the $T = 3$ surface lattice, which confirmed the good quality of the phases obtained by molecular averaging. Single isomorphous replacement (SIR) phases were calculated and an electron density map was computed with these phases and native amplitudes. The SIR map was averaged with fivefold noncrystallographic symmetry and phases were refined between 20 and 8 Å. Attempts were made to extend the phases to 6 Å, but the amplitudes were weak and the effective resolution of the map did not significantly improve. The CMV electron density described below was based on the SIR, phase-refined elec-

TABLE 2

A Summary of the FMA Derivative Data Set Collected on the Siemens Area Detector ($I > 3\sigma(I)$)

Resolution (Å)	Percentage of theoretically observable data	Number of unique reflections
99–50.0	28	8
50–40.0	52	15
40–30.0	68	55
30–20.0	64	212
20–17.0	58	168
17–15.0	56	192
15–13.0	52	314
13–11.0	50	544
11–10.0	48	446
10–9.0	42	580
9–8.0	32	703
Total: 99–8.0	40	5475

TABLE 3

Heavy Atom Sites for the FMA Derivative after Least-Squares Refinement of Heavy Atom Coordinates and Relative Occupancies with Fixed Temperature Factors of 20.0 (The Corresponding Peak Heights in Difference Fourier (DF) Maps Are Also Listed)

Sites	X (Å)	Y (Å)	Z (Å)	Relative occupancy	Height in DF
1	1.21	−8.47	113.38	1.11	1400
2	22.56	22.93	107.08	1.13	1400
3	41.98	−10.52	101.45	0.88	1000

tron density; hence it had no bias from the CCMV-based phasing model.

The distribution of the electron density in the X-ray map was similar to the EM image reconstruction (Fig. 1). The exterior radius along the quasi-sixfold axes was 144 Å. The density near the fivefold axes extended 3 Å further. Depressions were found close to the twofold and quasi-twofold axes. The electron density map for each subunit was consistent with a β -barrel motif. The long axis of the β -barrel domain was oriented in a roughly radial direction. An outstanding feature at this resolution was cylinder-like density around the threefold (quasi-sixfold) axes, in the interior of the protein shell (Fig. 1b). This density extended between 80 and 100 Å from the virus center and connected to the B and C subunits related by quasi-sixfold symmetry.

There are striking similarities between the CMV and the CCMV structures. The cryoEM image reconstruction for both viruses show similar pentamer and hexamer clustering of subunits, although there are some differences in the appearance of the capsomers. In CMV, the pentamers are sealed with density, in contrast to the pore in the CCMV pentamer. This difference may be due to the larger CMV coat protein size or to a difference in the orientation of the β -barrel.

The cylindrical density in CMV around the threefold axes (Fig. 1) formed a β -annulus. At 8 Å resolution, the CCMV map appears very similar in this region. In CCMV, residues 29 to 33 of the B and C subunits formed a β -hexamer structure (Speir *et al.*, 1995). The β -hexamer diameter was slightly larger in CMV than in CCMV. This would occur if the pitch of the β -strands forming the cylinder were less in CMV or if there were longer side chains.

The β -hexamer observed in CMV and CCMV is a variant of the β -annulus observed in many plant virus capsids. The arm domain connecting the N-terminal basic R-domain to the β -barrel domain has been visualized in the electron density for C subunits in several $T = 3$ plant viruses (Harrison, 1983) including Southern bean mosaic virus and tomato bushy stunt virus. The N-terminal arms of the three C subunits extend along an inner edge of the protein shell and loop around the threefold axes,

chlorosis, and aphid transmissibility (Palukaitis *et al.*, 1991; Perry *et al.*, 1994). In the mosaic-inducing CMV strains, a proline is present at amino acid 129; the chlorosis-inducing strains have either a serine or a leucine in this position (Shintaku, 1991). Aphid transmissibility is affected by changes at residues 129 and 162 (and perhaps 168) (Perry *et al.*, 1994). The sequence alignment suggests that the residues affecting chlorosis and transmissibility reside in loop regions of the structure. The sequence alignment suggests that residue 129 lies between the β E strand and the α EF helix and that residue 162 lies between the β G and α GH helix. In CCMV the β G- α GH loop is on the capsid interior, and the β E- α EF loop is on the surface.

For many $T = 3$ plant viruses, the N-terminal region of the coat protein contains a high concentration of basic amino acids, known as an internal R-domain. This domain is usually disordered in crystal structures (Harrison, 1983). It has been proposed that the basic amino acids are important for protein-RNA interactions and for the stability of the virion. The first 22 amino acids of the CMV coat protein have a net positive charge of +7. A remarkable feature is the high density of Arg residues (7 Arg's in residues 11–19), which probably interact with the RNA. There is evidence that the basic N-terminus of CCMV is α -helical after RNA binding (van der Graaf, 1991; van der Graaf *et al.*, 1991). An α -helix is unlikely in cucumoviruses, as this region contains proline residues in all three species. The stability toward ionic strength and pH is quite different for CCMV and CMV. Unlike the bromoviruses (Bancroft *et al.*, 1967), CMV does not undergo structural transitions and is accessible to ribonuclease; it has been characterized as a permanently "swollen" state.

The evidence for the structural similarity between CMV and CCMV is as follows: (1) A close evolutionary relationship between CMV and CCMV has been established by comparison of nonstructural proteins, including polymerase, helicase, putative methyltransferase, and the 3a (30K) protein (Gorbalenya *et al.*, 1989; Gorbalenya and Koonin, 1993; Davies and Symons, 1988; O'Reilly *et al.*, 1991). (2) The sequence alignment of the coat proteins of cucumoviruses and bromoviruses presented here indicates that CMV may fold into a β -barrel. (3) There is a similar arrangement of pentamers and hexamers in the cryoEM reconstruction. (4) The x-ray map indicates that the β -hexamer structure is present in CMV in the identical position to CCMV. (5) The X-ray map suggests that the CMV monomer is a β -barrel arranged with $T = 3$ quasi-symmetry in an orientation similar to that of CCMV.

The analysis suggests that physiochemical differences between CMV and CCMV result from substantial differences in primary structure superimposed on closely similar tertiary and quaternary structures. Preliminary structural results from alfalfa mosaic virus $T = 1$ particles and

crystalline TAV subunits suggest that this trend extends over the entire *Bromoviridae* family.

ACKNOWLEDGMENTS

We thank Peter Palukaitis for supplying virus inoculum for all three strains of CMV, as well as providing pure virus samples (Fny strain) for initial crystallization experiments. We thank the staff at the Cornell High Energy Synchrotron Source, Adam Zlotnick, and Jeffrey Speir for assistance in film data collection, and Tim Schmidt and Wladek Minor for assistance during area detector data collection. We also thank Jeffrey Speir for providing the CCMV atomic coordinates, Holland Cheng for the EM map conversion, Norm Olson for help in preparing Fig. 1, and Keith Perry, Sanjeev Munshi, M. R. N. Murthy, and Jin-bi Dai for helpful discussions. This work was supported by the National Institutes of Health Grant R01-GM54076 to John E. Johnson, by National Science Foundation Grant MCB9206305 to Timothy S. Baker and a Lucille P. Markey charitable grant to support the Purdue structural biology center. This is Paper No. 10491MB of The Scripps Research Institute.

REFERENCES

- Baker, T. S., Newcomb, W. W., Olson, N. H., Corvsert, L. M., Olson, C., and Brown, J. C. (1991). Structures of bovine and human papillomaviruses. *Biophys. J.* **60**, 1445–1456.
- Bancroft, J. B., Hills, G. J., and Markham, R. (1967). A study of the self-assembly process in a small spherical virus: Formation of organized structures from protein subunits *in vitro*. *Virology* **31**, 354–379.
- Bancroft, J. B. (1970). The self-assembly of spherical plant viruses. *Adv. Virus Res.* **16**, 99–134.
- Cheng, R. H., Olson, N. H., and Baker, T. S. (1992). Cauliflower mosaic virus: A 420 subunit ($T = 7$), multilayer structure. *Virology* **186**, 655–668.
- Davies, C., and Symons, R. H. (1988). Further implications for the evolutionary relationships between tripartite plant viruses based on cucumber mosaic virus RNA 3. *Virology* **165**, 216–224.
- Francki, R. I. B. (1968). Inactivation of cucumber mosaic virus (Q strain) nucleoprotein by pancreatic ribonuclease. *Virology* **34**, 694–700.
- Genetics Computer Group (1992). "Program Manual for the GCG Package, Version 7.2," November 1992, 575 Science Drive, Madison, WI, 53711.
- Gorbalenya, A. E., and Koonin, E. V. (1993). Comparative analysis of amino-acid sequences of key enzymes of replication and expression of positive-strand RNA viruses: Validity of approach and functional and evolutionary implications. *Sov. Sci. Rev. D Physiochem. Biol.* **11**, 1–84.
- Gorbalenya, A. E., Blinov, V. M., Donchenko, A. P., and Koonin, E. V. (1989). An NTP-binding motif is the most conserved sequence in a highly diverged monophyletic group of proteins involved in positive strand RNA viral replication. *J. Mol. Evol.* **28**, 256–268.
- Harrison, S. C. (1983). Virus structure: High-resolution perspectives. *Adv. Virus Res.* **28**, 175–240.
- Higgins, D. G., Bleasby, A. J., and Fuchs, R. (1992). CLUSTAL V: Improved software for multiple sequence alignment. *Comput. Appl. Biosci.* **8**, 189–191.
- Kabsch, W. (1988a). Automatic indexing of rotation diffraction patterns. *J. Appl. Crystallogr.* **21**, 67–71.
- Kabsch, W. (1988b). Evaluation of single-crystal X-ray diffraction data from a position-sensitive detector. *J. Appl. Crystallogr.* **21**, 916–924.
- Lot, H., Marrou, J., Quiot, J. B., and Esvan, C. (1972). Contribution à l'étude du virus de la mosaïque du concombre. II. Méthode de purification rapide du virus. *Ann. Phytopathol.* **4**, 25–38.
- Matthews, B. W. (1968). Solvent content of protein crystals. *J. Mol. Biol.* **33**, 491–497.

- McPherson, A. (1982). "Preparation and Analysis of Protein Crystals" Wiley, New York.
- Murphy, F. A., Faquet, C. M., Bishop, D. H. L., Ghabrial, S. A., Jarvis, A. W., Martelli, G. P., Mayo, M. A., and Summers, M. D. (1995). "Virus Taxonomy: Sixth Report of the International Committee on the Taxonomy of Viruses." Springer-Verlag, New York/Vienna.
- O'Reilly, D., Thomas, C. J. R., and Coutts, R. H. A. (1991). Tomato aspermy virus has an evolutionary relationship with other tripartite RNA plant viruses. *J. Gen. Virol.* **72**, 1–7.
- Olson, A. J., Bricogne, G., and Harrison, S. C. (1983). Structure of tomato bushy stunt virus IV. The virus particle at 2.9 Å resolution. *J. Mol. Biol.* **171**, 61–93.
- Palukaitis, P., Roossinck, M. J., Shintaku, M. H., and Sleat, D. E. (1991). Mapping functional domains in cucumber mosaic virus and its satellite RNAs. *Can. J. Plant Pathol.* **13**, 155–162.
- Perry, K. L., Zhang, L., Shintaku, M. H., and Palukaitis, P. (1994). Mapping determinants in cucumber mosaic virus for transmission by *aphiz gossypii*. *Virology* **205**, 591–595.
- Rossmann, M. G. (1976). The refinement of heavy-atom parameters in the presence of non-crystallographic symmetry. *Acta Crystallogr. Sect. A* **32**, 774–777.
- Rossmann, M. G. (1979). Processing oscillation diffraction data for very large unit cells with an automatic convolution technique and profile fitting. *J. Appl. Crystallogr.* **12**, 225–235.
- Rossmann, M. G., and Blow, D. M. (1962). The detection of sub-units within the crystallographic asymmetric unit. *Acta Crystallogr.* **15**, 24.
- Rossmann, M. G., Leslie, A. G. W., Abdel-Meguid, S. S., and Tsukihara, T. (1979). Processing and post-refinement of oscillation camera data. *J. Appl. Crystallogr.* **12**, 570–581.
- Rost, B., and Sander, C. (1993). Prediction of protein secondary structure at better than 70% accuracy. *J. Mol. Biol.* **232**, 584–599.
- Rost, B., and Sander, C. (1994). Combining evolutionary information and neural networks to predict protein secondary structure. *Proteins* **19**, 55–72.
- Rost, B., Sander, C., and Schneider, R. (1994). PHD—An automatic mail server for protein secondary structure prediction. *Comp. Appl. Biosci.* **10**, 53–60.
- Sehnke, P. C., and Johnson, J. E. (1993). Crystallization and preliminary X-ray characterization of tobacco streak virus and a proteolytically modified form of the capsid protein. *Virology* **196**, 328–331.
- Speir, J. A., Munshi, S., Wang, G., Baker, T. S., and Johnson, J. E. (1995). Structures of the native and swollen forms of cowpea chlorotic mottle virus determined by X-ray crystallography and cryo electron microscopy. *Structure* **3**, 63–78.
- Speir, J., Munshi, S., Baker, T. S., and Johnson, J. E. (1993). Preliminary X-ray data analysis of crystalline cowpea chlorotic mottle virus. *Virology* **193**, 234–241.
- Shintaku, M. (1991). Coat protein gene sequences of two cucumber mosaic virus strains reveal a single amino acid change correlating with chlorosis induction. *J. Gen. Virol.* **72**, 2587–2589.
- Smith, T. J., Olson, N. H., Cheng, R. H., Chase, E. S., and Baker, T. S. (1993). Structure of a human rhinovirus-bivalently bound antibody complex: Implications for viral neutralization and antibody flexibility. *Proc. Natl. Acad. Sci. USA* **90**, 7015–7018.
- van der Graaf, M. (1991). Conformation and mobility of the RNA-binding N-terminal part of the intact coat protein of cowpea chlorotic mottle virus. A two-dimensional proton nuclear magnetic resonance study. *J. Mol. Biol.* **220**, 701–709.
- van der Graaf, M., van Mierlo, C. P. M., and Hemminga, M. A. (1991). Solution conformation of a peptide fragment representing a proposed RNA-binding site of a viral coat protein studied by two-dimensional NMR. *Biochemistry* **30**, 5722–5727.
- Yusibov, V., Kumar, A., North, A., Johnson, J. E., and Loesch-Fries, L. S. (1996). Purification, characterization, virion assembly, and crystallization of alfalfa mosaic virus coat protein expressed in *Escherichia coli*. *J. Gen. Virol.* **77**, 567–573.